

Mapping tropical forest cover and deforestation using synthetic aperture radar (SAR) images

M. Mahmudur Rahman ·
Josaphat Tetuko Sri Sumantyo

Received: 26 August 2009 / Accepted: 27 June 2010 / Published online: 23 July 2010
© The Author(s) 2010. This article is published with open access at Springerlink.com

Abstract The changes in forest cover in many parts of the world lead to increase the accumulation of atmospheric carbon and thus accelerate the process of global warming. Optical remote sensing has been used to map and quantify deforestation but its application is limited because of the presence of cloud coverage on the images. Recent availability of several space-borne synthetic aperture radar (SAR) missions has widened the scope of utilizing radar images for monitoring of forest cover change. The objective of this investigation is to examine the capability of SAR data to assess and map deforestation. The study area is located at the tropical forest region of southeastern Bangladesh. Shuttle Imaging Radar-C (SIR-C) data of 1994 and Advanced Land Observation Satellite (ALOS) PALSAR data of 2007 were used in this study. ALOS PALSAR data were orthorectified with Shuttle Radar Topographic Mission digital elevation model data. Image to image geometric registration was done between the two SAR scenes. Study area was clipped and separated as subsets. SIR-C data (L- and C-bands) was in dual polarization (HH and HV) and PALSAR (L-band) was in quad-polarization (HH, HV, VH, and VV). Five different categories of land covers (forest, upland soil/shrubs, lowland

soil, settlements, and water/wetlands) were recognized on both SAR scenes. An additional class representing forest re-growth could be identified only on SIR-C image. Both the images were classified using maximum likelihood algorithms. The classification accuracy was computed from the randomly selected independent validation pixels. The accuracy for forest is more than 83% except users accuracy computed for PALSAR image. Forest was reduced from 18,000 to 13,800 ha in the region during the study period. The results of this study will be useful for understanding the applicability of SAR to map and quantify forest cover changes in the tropics.

Keywords Forest · Deforestation · Mapping · SIR-C · PALSAR

Background

Quantitative assessments of forests and changes in forest coverage are essential since forest area in the world is changing at an alarming rate. Net reduction of global forest coverage in the period of 2000–2005 is 7.3 million hectares per year, an area about the size of Panama or Sierra Leone though it is slightly declined compared to the last decade (8.9 million ha per year during the period in 1990–2000) (FAO 2006). The changes in forest coverage will play a role in the terrestrial carbon flux. Deforestation and forest degradation will release locked carbon from forest to the atmosphere and threatened our planet to be warmer, which might have many adverse impacts on our living systems.

Synthetic aperture radar (SAR) has been used to quantify forest cover (Ranson and Sun 1994; Dobson et al. 1996; Pierce et al. 1998; Simard et al. 2000) and forest cover change (Ranson and Sun 1997; Rignot et al. 1997; Saatchi

M. M. Rahman (✉) · J. T. S. Sumantyo
Microwave Remote Sensing Laboratory,
Center for Environmental Remote Sensing, Chiba University,
1-33, Yayoi, Inage,
Chiba 263-8522, Japan
e-mail: mahmud@sparrso.gov.bd

Present Address:
M. M. Rahman
Bangladesh Space Research and Remote Sensing Organization
(SPARRSO),
Agargaon, Sher-E-Bangla Nagar,
Dhaka 1207, Bangladesh

et al. 1997). SAR data used in those studies are from experimental (Ranson and Sun 1997; Rignot et al. 1997; Saatchi et al. 1997) and commercial SAR missions (Fransson et al. 2007; Santos et al. 2008). SAR has the capability of acquiring data throughout the year irrespective of cloud coverage, while optical sensing is often affected by the presence of cloud cover in the desired seasons and time. Several newly launched satellites are in operation with full polarization SAR on-board to collect radar data including RADARSAT-2 (Canada), TerraSAR-X (Germany), and Advanced Land Observation Satellite (ALOS) PALSAR (Japan) and widen the opportunity of forest monitoring in the preferred season and time using multi-polarized SAR data. Only few studies used these datasets for forest cover mapping (Rahman and Sumantyo 2008) and deforestation studies (Rahman and Sumantyo 2009).

This investigation examines the applicability of SIR-C and PALSAR data for deforestation and land cover mapping. The objectives of this investigation are to (1) examine multi-polarized SAR data for forest cover mapping and change assessments and (2) analyze the response of various land covers on SAR data acquired in different polarizations.

Study area and datasets

Major part of the study area is located in the southeastern corner of Bangladesh belongs to the administrative districts of Cox's Bazar and Bandarban and a small portion is in Myanmar. It covers 92°03' to 92°12' E longitude and 21°

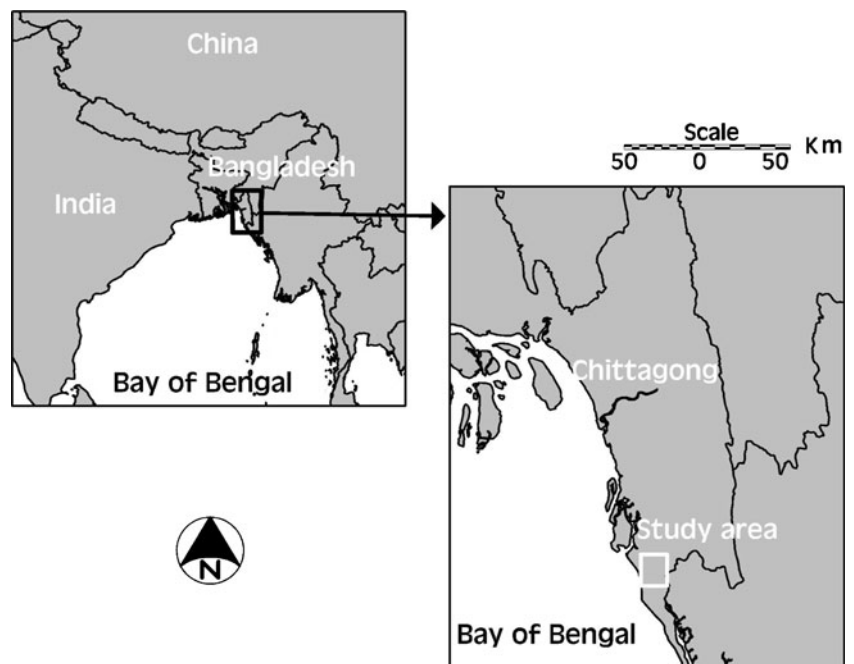
18' to 21°29' N latitude (Fig. 1). The area is characterized by sub-tropical monsoon climate where it has three distinct seasons: pre-monsoon hot season (March–May), monsoon (June–October), and cool dry winter (November–February). Heavy rainfall is concentrated in the monsoon season and about 80% of the annual rainfall occurs in the few months of monsoon period.

The forests of the study area are classified as tropical wet evergreen forests and tropical semi-evergreen forest (Champion et al. 1965). Tropical wet evergreen forest is characterized by the presence of a considerable proportion of evergreen trees in upper canopy. The Dipterocarps are the characteristic feature of evergreen stratum. A certain amount of deciduous species, *Anacardaeous* and *Swintonia* is often present.

On the semi-evergreen forest the dominance of appreciable proportion of deciduous species in the top canopy is noticed. The canopy is correspondingly lighter during the period of minimum rainfall (November to March) because of shedding leaves. Epiphytes, climbers, and bamboos are often present in the lower canopy, which later in some extent are replaced by canes and palms in climax evergreen formation.

Since all the accessible areas were transformed to shifting cultivation, virgin forests are seldom noticed. Present crop mostly consists of secondary re-growth, which is still in the process of succession to the climax evergreen type. This process of succession is often influenced by the continuous human disturbance and thus leads to a drier scrubby forest or to a savannah in many areas (Khan 1979).

Fig. 1 Location of the study area



Dual polarization (HH and HV) SIR-C data with L- and C-bands on 17 April 1994 and ALOS PALSAR (L-band) quad-polarization data (HH, HV, VH, and VV) on 9 March 2007 have been selected for this study (details in Table 1). Additional optical data, Landsat Thematic Mapper (TM) of 7 February 1992 and 13 February 2006 and Enhanced Thematic Mapper Plus (ETM+) image of 7 February 2001 were used additionally to assist in image interpretation procedures.

Methodology

Level 1.5 ALOS PALSAR data was procured from Remote Sensing Technology Center (RESTEC) of Japan. Data was orthorectified using Shuttle Radar Topography Mission digital elevation model and image header information. SIR-C radar data was downloaded from United States Geological Survey website. Data was extracted in normalized radar cross-section (NRCS, often termed as backscattering coefficients) by applying appropriate calibration coefficients. This image was geo-coded from header information. Both ALOS PALSAR and SIR-C data were in ground range and processed by standard software used in RESTEC and Jet Propulsion Laboratory, respectively. In order to reduce the geometric distortions between two scenes it was further rectified with PALSAR image using first-order polynomial function. Speckle noises on both of the datasets were reduced by applying Lee-sigma filter (3×3).

Five categories of land covers (forest, upland soil/shrubs, lowland soil, settlements, and water/wetlands) were interpreted on both SIR-C and PALSAR; an additional category namely forest re-growth was only detected on SIR-C image. Both SAR/Landsat image interpretation and ground verifications assisted in defining the land cover types. SAR images were classified using a supervised training method by applying maximum likelihood algorithms. ERDAS IMAGINE software was used in SAR image processing. For each category of land covers several training

Table 2 Number of training pixels used in supervised classification

Class	Number of training pixels	
	SIR-C	PALSAR
Forest	40,447	20,292
Forest re-growth	3,699	–
Upland soil/shrubs	2,523	19,472
Lowland soil	12,605	1,642
Settlements	4,142	4,870
Water/wetlands	4,977	2,297

pixel-sets with fairly homogenous areas were selected (details of training pixels are presented in Table 2). Ground verification of Landsat scene was earlier done in several field sampling missions during 1998–2004.

Classification accuracy was computed from the independent sample plots; 300 samples were randomly selected both on the classified SIR-C and ALOS PALSAR scenes for validation purpose. The total area of the classified maps was considered for accuracy assessments. Validation result was checked using Landsat (1992 and 2006) and SAR images. Since the category of forest re-growth could only be recognized on SIR-C image the class was merged with forest in order to harmonize the land cover classification between two SAR scenes prior to change computation. The changes in forest covers were estimated in change map and matrix.

ALOS PALSAR 16-bit intensity image was converted to NRCS prior to quantitative analysis of NRCS for different land covers. Following formula (Anon 2009) was used:

$$\text{NRCS} = 10 \log_{10}(\text{DN})^2 + \text{CF} \quad (1)$$

Where, DN is the 16-bit digital number of amplitude image (format 1.5) and CF is the conversion factor (−83.0) obtained from image header.

Table 1 Description of input data used in this study

Sensor	Band	Polarization	Orbital direction	Radar frequency (GHz)	Incidence angle (°)	Wavelength (μm)	Pixel size (m)
SIR-C	C	HH	Descending	5.304	52.3	375–750	12.5
		HV					
	L	HH		1.254			
		HV					
ALOS PALSAR	L	HH	Ascending	1.270	21.5	1,500–3,000	12.5
		HV					
		VH					
		VV					

Table 3 Land cover categories and SAR interpretation remarks (PALSAR: VV—red, VH—green, and HV—blue; SIR-C: CHV—red, CHH—green, and LHV—blue)

Land cover types	Spectral class combinations	Physical characteristics	Interpretation remarks	
			SIR-C	PALSAR
Forest	Natural forest	Tropical wet evergreen and semi-evergreen forests	Mixture of light gray and purple	Light cyan
	Plantations	Planted with teak, dipterocarps, and other long-rotation species		
Forest re-growth	Young forest	Forms after removal of primary forests	Purple	–
	Bamboo		Scattered distribution in the forest	
Upland soil/shrubs	Upland soil	Bare soil on the hill slopes, resulted after forest clearings	Blue	Dark brown color
	Sandy soil on the riverbank	Riverbank soil often used for vegetable cropping		
	Shrubs	Shrubs (vegetations formed after forest clearing and are usually 1–3 m height)		
Lowland soil	Bare soil (lowland)	Rice fields	Green. Sometimes mixed with yellow	Red
				Appears in black if soil is flooded
Settlements	Houses and man-made structures	Rural homesteads	Tan	White
	Trees and other crops			
Water/wetlands	Water	Permanent water	Dark tone	Dark tone
	Wetlands	Seasonally inundated areas		

Results and discussion

Different land covers were interpreted on SAR images (SIR-C and PALSAR) and the details of interpretation remarks are presented in Table 3 and Fig. 2.

The differences of NRCS values for different land covers are more distinct in L-band than in C-band with a high incidence angle (52.3°) on SIR-C image (Fig. 3). NRCS is higher in co-polarization (HH) than cross-polarization (HV) in both C- and L-bands. The difference of mean NRCS between forest and upland soil/shrubs (the class often formed after deforestation) is 1.6 dB in C band (HH and HV) and 4.6 (HH) and 7.2 dB (HV) in L-band. The largest numerical difference of NRCS in L-band HV polarization (LHV) indicates the best identification possibility of deforestation hotspots using this band and the polarization when removal of forest results upland soil/shrubs category. Mean NRCS of upland soil/shrubs is lower than lowland soil in co-polarization but higher in cross-polarization both in C- and L-bands. It means that the first derivative of NRCS between these two polarizations or a numerical difference index could be a useful indicator to separate between these categories.

On PALSAR scene, NRCS is higher in co-polarizations (HH and VV) than cross-polarizations (HV and VH) in a

lower incidence angle (21.5° ; Fig. 4). Forest is distinguishable from upland soil/shrubs, especially in cross-polarization where differentiation between these two classes are distinct; mean NRCS of forest decreases about 6 dB after converted to upland soils/shrubs. But in co-polarization mean NRCS declines slightly, only about 1–2 dB. The differentiation between upland soil/shrubs and lowland soil is difficult in cross-polarization, but in co-polarization NRCS is higher in lowland soil than upland soil/shrubs. Water/wetlands are separable in all different polarizations; NRCS of this class is identically lower than other land cover categories in all different polarizations because flooded soil acts as a mirror reflector on SAR signals and consequently appears darker on the image.

NRCS of forest is slightly lower in SIR-C than PALSAR scene in LHH and LHV; the mean difference is 1 to 2 dB. This may be the result of differences in incidence angle or the changes in forest stocking (forest degradation or amelioration). The largest difference of NRCS between these two datasets is for lowland soil in HH polarization; the mean difference is 9.3 dB.

The magnitude of radar backscatter on a forest canopy depends upon radar wavelength, polarization and incidence angle as well as terrain conditions and canopy parameters.

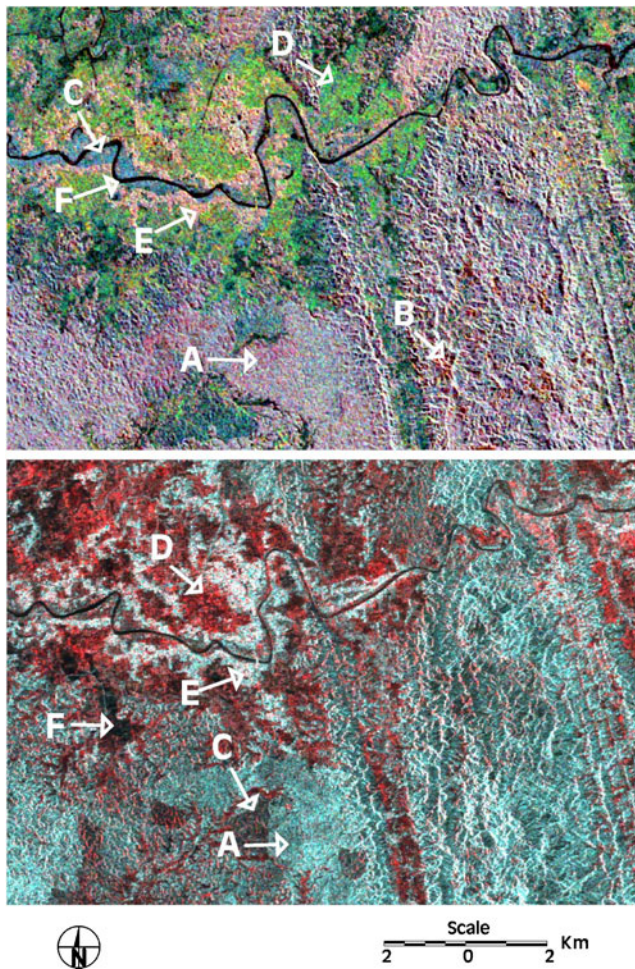


Fig. 2 SIR-C (CHV—red, CHH—green, and LHV—blue) and ALOS PALSAR raw images (LVV—red, LVH—green, and LHV—blue). *A* Forest, *B* forest re-growth, *C* upland soil/shrubs, *D* lowland soil, *E* settlements, and *F* water/wetlands

The total backscatter from forest land includes response from several components: (1) crown volume scattering (dominant in C-band), (2) backscattering from secondary branches and trunks (dominant in L-band), (3) backscattering from ground, especially if canopy is sparse (for L-band) or there is a gap in the canopy (both C- and L-bands), (4) crown-ground (mostly in C-band) or trunk-ground (L-band) backscattering, often termed as double bounce (can be in both direction such as ground-trunk). Presence of understory, which is often a common phenomenon in a multi-storied tropical forest, may have strong influence as well. When there is an interaction with ground surface roughness, soil moisture, incidence angle/slope will have an important effect on SAR signals. Backscattering from beneath the canopy may be attenuated by the canopy itself when SAR signals return back to the sensor (adapted from Leckie and Ranson 1998).

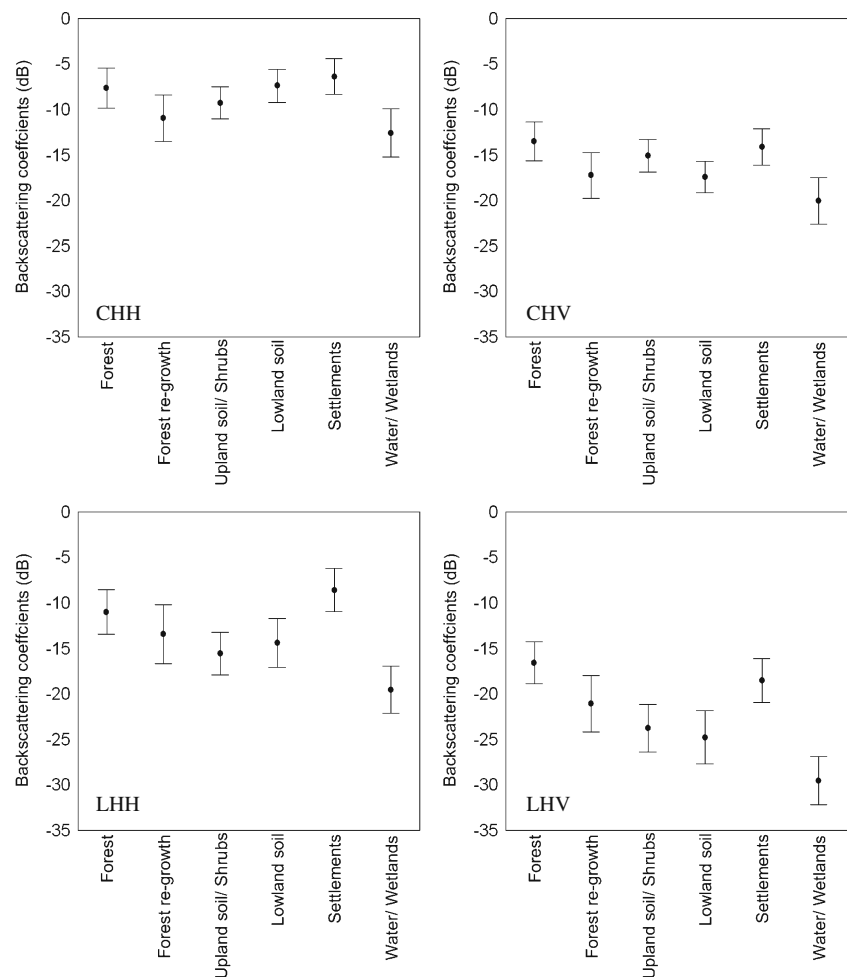
The overall classification accuracy for SIR-C and PALSAR images are around 65% (details in Table 4). Similar accuracy was also reported in the other studies. Bijker (1997) reported a classification accuracy of 60–70% for forest, secondary vegetation, pastures, and natural grasslands in the Colombian Amazon forest region using multi-temporal ERS SAR data. Wu (1984) achieved a classification accuracy of 59% in Kershaw County, South Carolina, using X-band SAR with three polarizations (HH, HV, and VV). The study also reported 67% accuracy for Baldwin County, Alabama, using SAR-A data. However, Saatchi et al. (1997) obtained higher accuracy for mapping deforestation and land use in Amazon Rainforest using SIR-C image. The study reported the accuracy of 72% for five classes of land cover and 87% for three classes. It should be kept in mind that the land covers in the Amazon region are often continuous up to several kilometers but in the South Asian regions where the study area of this investigation belongs are often fragmented and intermixed with each other.

The classification of forest achieves high accuracy, especially on SIR-C images, which ranges from 83% to 87%. Producers accuracy of this class on PALSAR image is higher (89%) though users accuracy is low (57%). It means that if we could use only two classes, forest and non-forest classification, accuracy could be increased. One can examine hybrid classifier (details can be found in Lillesand et al. 2008) where spectral subclasses are aggregated and classified using maximum likelihood algorithms and finally, merged to the original classes. Bauer et al. (1994) applied hybrid classifiers for optical imageries.

Higher classification accuracy could not be achieved because of several reasons. Sometimes it becomes difficult to separate between lowland soil and upland soil using SAR/Landsat imagery. One can classify these spectral subclasses and later merged together to distinguish soil category. The class water/wetlands is contemporary in the study region; the extent of this class changes with seasons. There are 1–2 months of difference between the SAR and Landsat image acquisition. There are 1–2 year's difference between SAR images and Landsat data as well. Any changes in the land covers during this period need to be carefully explored. It is also often difficult to differentiate between forest re-growth and scrubby re-growth using Landsat data. Settlements are often difficult to interpret on the Landsat images.

Forest cover change is presented in comparative maps (Fig. 5) as change matrix (Table 5). This matrix shows not only the quantity but also the dimensions of changes. The rows and the columns present the land cover statistics in historical and recent times, respectively. Every cell in the matrix represents both the origins and destinations of classes. The stable classes are the italicized cell entries. In

Fig. 3 SIR-C NRCS for different land cover classes. High and low values are the mean and plus/minus of standard deviation



1994, forest area was estimated at around 18,000 ha, which was reduced to 13,800 in 2007 (decline about 23%). Of the deforested areas the major portion (6,100 ha) was converted to upland soil/shrubs. The scattered distributions of deforested areas are noticed in many locations and are prominent in the central south and southwestern region.

It should be kept in mind that the deforestation figures reported in this study are also influenced in the classification accuracy of historical and recent forest cover maps. The classification accuracy (particularly users accuracy) for forest in the recent image is lower than the historical image. This is understandable since historical image (SIR-C) contains both L- and C-bands while the recent image (PALSAR) has only L-band. Further studies should be directed to increase the accuracy of forest classification using PALSAR imageries.

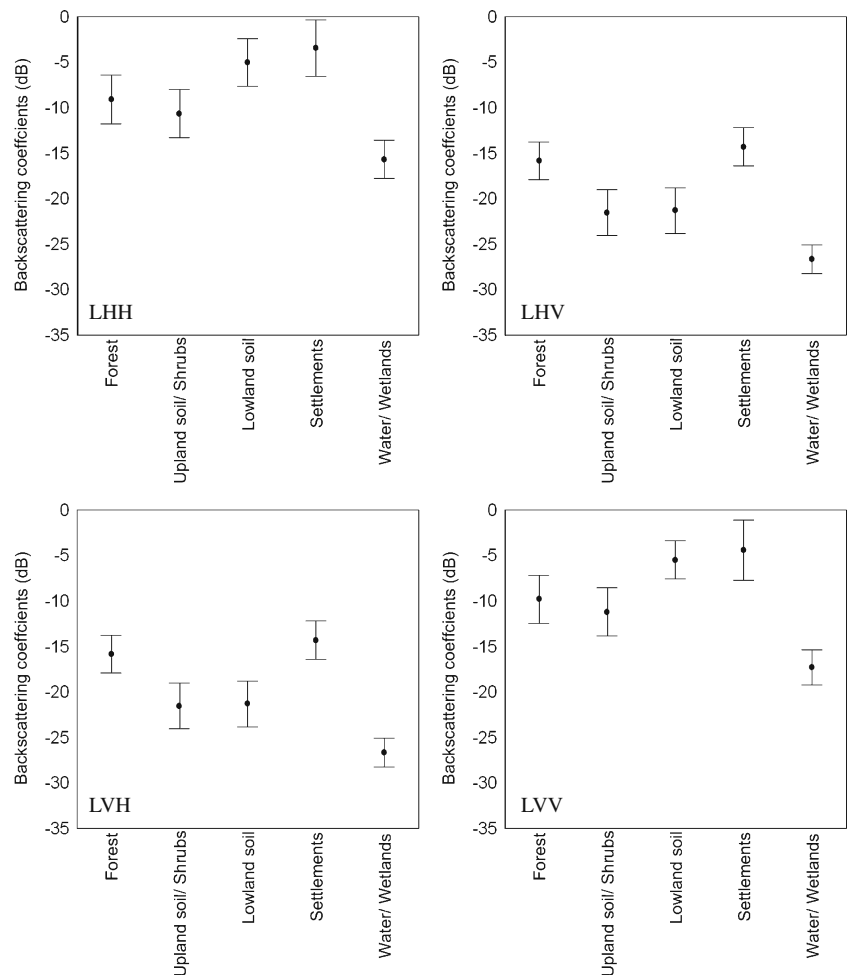
Current study estimated forest cover change using post-classification technique. Post-classification change detection has the advantage that datasets can be used from different sensors or bands since an interpreter has the flexibility to classify the images independently. The SAR

datasets used in this study are from different sensors: they have different band combinations (partially overlapping), different incidence angle and opposite orbital direction. Orbital direction and incidence angle will have an effect on viewing geometry. Image-to-image radiometric normalizations may be a common technique to reduce mis-matching errors of multi-sensor optical images (further elaboration in Suits et al. 1988), but their application on SAR image needs to be further investigated.

Conclusion

The results presented in this study suggest that dual polarization and quad-SAR data can suitably be used for the mapping of land covers and detect any changes. Forest can be separated reasonably well from other land covers and achieve accuracy more than 83% (83% producers and 87% users accuracy using SIR-C images (L- and C-bands, dual-polarizations)). Similar results were also achieved for producers accuracy (89%)

Fig. 4 ALOS PALSAR NRCS for different land cover classes. High and low values are the mean and plus/minus of standard deviation



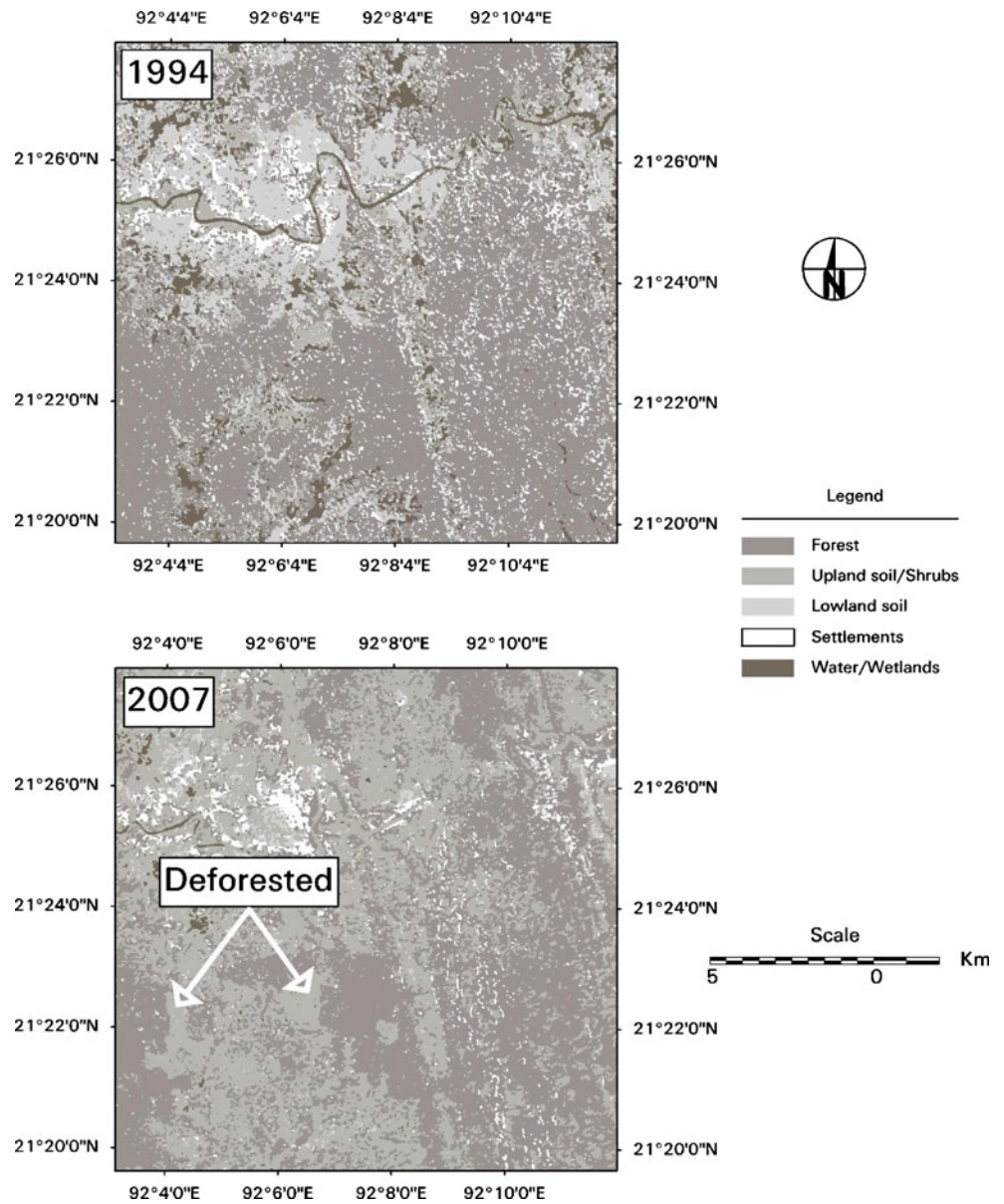
using quad-polarization L-band ALOS PALSAR data. The users accuracy (only 57%) in the latter scene indicates that further studies should be conducted to explore any possibility to increase it. From the graphs presented in this study, L-band shows more differentiation

ability among various land covers than C-band and the distinction among different land covers is prominent in cross-polarization than in co-polarization. Finally, the study region has lost around 23% of forest during last 13 years, which mostly converted to bare soil or shrubs.

Table 4 Accuracy of land cover classification computed from independent validation pixels

Class	SIR-C		PALSAR	
	Producers (%)	Users (%)	Producers (%)	Users (%)
Forest	83.17	86.60	88.73	57.27
Forest re-growth	96.30	36.62	–	–
Upland soil/shrubs	30.77	58.82	61.94	74.11
Lowland soil	62.71	77.08	67.86	67.86
Settlements	68.42	52.00	42.42	46.67
Water/wetland	51.72	60.00	52.94	90.00
Overall statistics	Accuracy, 65.00% Kappa, 0.5628		Accuracy, 65.67% Kappa, 0.5226	

Fig. 5 Forest cover maps (1994 and 2007) of Southern Chittagong (south-eastern corner belongs to Myanmar). Classified SIR-C image on the top and ALOS PALSAR on the bottom



This study is a pioneer effort to utilize quad-polarization PALSAR polarimetric data to assess its effectiveness for forest cover mapping and deforestation assessments in the tropics. Further studies should be concentrated on the utilization of

SAR magnitude data in different incidence angle and also SAR phase information to compute coherence images in different polarizations to investigate the higher separation capabilities of forest and other land covers.

Table 5 Forest cover change matrix 1994–2007 (area in ha)

	2007					
1994	Forest	Upland soil/shrubs	Lowland soil	Settlements	Water/wetlands	Total (1994)
Forest	10,185	6,100	429	1,206	74	17,994
Upland soil/shrubs	1,160	2,027	242	169	75	3,673
Lowland soil	739	3,417	632	159	192	5,139
Settlements	1,297	823	86	446	8	2,660
Water/wetlands	410	1,826	217	61	138	2,652
Total (2007)	13,791	14,193	1,606	2,041	487	32,118

Acknowledgments Japan Society for the Promotion of Science (JSPS) is acknowledged for the post-doctoral fellowship grant to the first author. The authors would like to thank JSPS for Grant-in-Aid for Scientific Research (no. 1907023). SIR-C data was downloaded from United States Geological Survey websites.

Open Access This article is distributed under the terms of the Creative Commons Attribution Noncommercial License which permits any noncommercial use, distribution, and reproduction in any medium, provided the original author(s) and source are credited.

References

- Anon (2009) ALOS PALSAR Frequently asked questions. ALOS-PALSAR-FAQ-001. ESRIN Contract No.20700/07/I-OL. Available at: <http://earth.eo.esa.int/pcs/alos/palsar/userinfo/ALOS-PALSAR-FAQ-001.3.pdf> (accessed April 19, 2010)
- Bauer ME, Burk TE, Ek AR, Coppin PR, Lime SD, Walsh TA, Walters DK, Befort W, Heinzen DF (1994) Satellite inventory of Minnesota forest resources. *Photogramm Eng Rem Sens* 60(3):287–298
- Bijker W (1997) Radar data for rain forest: a monitoring system for land cover change in the Colombian Amazon. Doctoral thesis, ITC, Enschede, the Netherlands, 189p.
- Champion HG, Seth SK, Khattak GM (1965) Forest Types of Pakistan. Pakistan Forest Institute, Peshawar
- Dobson MC, Pierce LE, Ulaby FT (1996) Knowledge-based land-cover classification using ERS-1/JERS-1 SAR composites. *IEEE Trans Geosci Rem Sens* 34(1):83–99
- FAO (2006) Global Forest resources assessment 2005: Progress towards sustainable forest management. FAO Forestry Paper 147. FAO, Rome
- Fransson JES, Magnusson M, Olsson H (2007) Detection of forest changes using ALOS PALSAR satellite images. In *Proceedings of IEEE Geoscience and Remote Sensing Symposium (IGARSS)*, pp. 2330–2333. doi:10.1109/IGARSS.2007.4423308
- Khan SA (1979) Revised working plan for the forests of Chittagong Division (for the years 1978–79 to 1987–88). Volume 1. Forest Department, Government of Bangladesh, Dhaka.
- Leckie DG, Ranson KJ (1998) Forestry applications using imaging SAR. In: Henderson FM, Lewis AJ (eds) *Principles and application of imaging radar—manual of remote sensing*. 3rd edn. Vol. 2. Wiley, New York
- Lillesand TM, Kiefer RW, Chipman JW (2008) *Remote sensing and image interpretation*. Wiley, New York
- Pierce LE, Bergen KM, Dobson MC, Ulaby FT (1998) Multitemporal land-cover classification using SIR-C/X-SAR imagery. *Rem Sens Environ* 64:20–33
- Rahman MM, Sumantyo JTS (2009) Mapping Forest Cover Change in the Amazonia Using Synthetic Aperture Radar (SAR) Images. 33rd International Symposium on Remote Sensing of Environment. May 4–8, 2009, Stresa, Italy.
- Rahman MM, Sumantyo JTS (2008) ALOS PALSAR Data for Tropical Forest Interpretation and Mapping. In: Jun C, Jie J, Genderen J (eds). *International Archives of the Photogrammetry, Remote Sensing and Spatial Information Sciences*. Volume XXXVII Part B7-1. pp. 185–189. ISPRS, Beijing
- Ranson KJ, Sun G (1994) Northern forest classification using temporal multifrequency and multipolarimetric SAR images. *Rem Sens Environ* 47(2):142–153
- Ranson KJ, Sun G (1997) An evaluation of AIRSAR and SIR-C/X SAR images for mapping Northern Forest Attributes in Main, USA. *Rem Sens Environ* 59:203–222
- Rignot E, Salas WA, Skole DL (1997) Mapping deforestation and secondary growth in Rondonia, Brazil, using imaging radar and Thematic Mapper data. *Rem Sens Environ* 59:167–179
- Saatchi SS, Soares JV, Alves DS (1997) Mapping deforestation and landuse in Amazon Rainforest by using SIR-C imagery. *Rem Sens Environ* 59:191–202
- Santos JR, Mura JC, Paradella WR, Dutra LV, Gonçalves FG (2008) Mapping recent deforestation in the Brazilian Amazon using simulated L-band MAPSAR image. *Int J Remote Sens* 29(16):4879–4884
- Simard M, Saatchi SS, Grandi GD (2000) The use of decision tree and multiscale texture for classification of JERS-1 SAR data over tropical forest. *IEEE Trans Geosci Rem Sens* 38(5):2310–2321
- Suits G, Malila W, Weller T (1988) Procedures for using signals from one sensor as substitutes for signals of another. *Rem Sens Environ* 25:395–408
- Wu ST (1984) Analysis of synthetic aperture radar data acquired over a variety of land cover. *IEEE Trans Geosci Rem Sens* GE-22:550–557